JOURNAL OF SOLID STATE CHEMISTRY 59, 168–173 (1985)

Preparation of $LiVO_2$ Crystals

T. A. HEWSTON AND B. L. CHAMBERLAND

Department of Chemistry, The University of Connecticut, Storrs, Connecticut 06268

Received December 10, 1984; in revised form February 1, 1985

The synthesis of $LiVO_2$ crystals exhibiting two different morphologies is reported. Black hexagonal platelet-type and octahedral-like dendritic crystals were obtained using a fused-salt electrolytic method. DSC, TGA, magnetic susceptibility, and X-ray diffraction data are presented. Weak reflections observed in X-ray precession photographs of the platelets indicate a hexagonal superstructure with a unit cell $a = 9.838(4)$ Å $= 2\sqrt{3}a'$, where $a' = 2.84$ Å, and $c = 14.755(6)$ Å. Observed systematic absences are consistent with the space groups $P6_222$ and $P6_422$. The dendrites appear to be a pseudocubic phase with a face-centered unit cell, $a = 8.31(1)$ Å.

Introduction

The compound $LiVO_2$ was first reported in 1954 by Rüdorff and Becker (*1*). X-Ray powder diffraction analysis indicated a structure isotypic with that of α-$NaFeO_2$. This is an ordered rock salt-type structure in which the two different cations are segregated on alternate (111) cubic planes, an arrangement which lowers the crystal symmetry to trigonal. $LiVO_2$ was found to undergo an unusual phase transition near 200°C accompanied by anomalies in calorimetric, magnetic, electrical, and structural properties (*2–6*). A mechanism for the transformation has been suggested which is based on the formation of metal-to-metal bonds within the vanadium planes (*2, 3, 5, 6*). The transition has been described as first order according to the observation of hysteresis (*5*), and a discontinuity in the unit cell parameters at the transition temperature has been reported ($a = 2.83$ to 2.89 Å, $c = 14.87$ to 14.48 Å) (*5*). The change in unit cell corresponds to a 1.6% increase in volume upon heating through the transition temperature; however, no change in crystallographic symmetry was observed, as would be expected upon changes in V–V bond distances.

Efforts to fully characterize $LiVO_2$ and the nature of its phase transition have been hampered by the unavailability of single crystals—this compound has heretofore been obtained only as a black powder. Attempts to prepare single crystals using high-pressure techniques produced a metastable form of $LiVO_2$ with the atacamite-type ordered rock salt structure (*7*). This structure type has also been found for a polymorph of $LiTiO_2$ prepared by lithiation of spinel-type $LiTi_2O_4$ with *n*-butyl lithium under ambient conditions (*8*). The present report describes the synthesis and characterization of two types of $LiVO_2$ crystals using fused-salt electrolysis. In a short note, Andrieux and Bozon (*9*) reported the use of a similar method to produce black octahedral crys-

0022-4596/85 $3.00

tals with the formula $2V_2O_3 \cdot Li_2O$. A statistical rock salt-type structure with cation vacancies was claimed with a unit cell edge of 4.10 Å.

Experimental Methods

The crystal growth apparatus consisted of a crucible-type furnace, a dc power supply, and a decade resistance box which served as a current limiter. The anode (+) and cathode (−) were carbon rods placed against the outside wall of a SiC crucible, and immersed centrally in the molten flux, respectively. The voltage was monitored directly across the two electrodes with a volt-ohm-milliammeter, and the current was measured with an in-line galvanometer. In a typical run, 2.4 g LiOH, 3.0 g V_2O_5, and 6.0 g LiCl were ground together, packed into a SiC crucible, and dried at 110–120°C. The crucible was then placed in the furnace and heated slowly to 650°C. After the flux was fully molten the temperature was raised to 800°C, the electrodes were positioned, and power was applied. The experiments were terminated by solidification of the flux around the cathode and/or breakage of one or both of the carbon electrodes caused by corrosion. A mixture of black crystals containing hexagonal platelets approximately 0.5 mm across and small black octahedral-like dendrites (0.05–0.10 mm on an edge) was obtained by applying 2.8 V/1.0 A for 3 hr at 800°C. In another experiment only larger octahedral-like dendrites 0.1–0.2 mm on an edge were obtained by using a reduced current of 0.1–0.5 A at 3.0 V for 7 hr at 800°C. Products were separated from the flux by leaching with 1 *M* HCl.

X-Ray diffraction patterns were obtained with filtered copper radiation using a Debye–Scherrer camera for powdered samples and a Gandolfi camera for crystals. Unit cell dimensions were calculated using a least-squares refinement program. Precession data were obtained with a Supper camera and filtered molybdenum radiation. Photographs of the crystals were obtained with a scanning electron microscope.

Thermal profiles were obtained with a thermal analyzer equipped wiht a DSC cell and a TGA module. DSC analyses were performed at 10°/min under a flowing inert gas (N_2 or Ar, 0.1 SCFH). Thermogravimetric analysis under flowing oxygen was carried out to determine the oxidation state of vanadium in the samples, and was based on the quantitative conversion of $LiVO_2$ to $LiVO_3$ above 800°C. The TGA residue was checked using X-ray diffraction—all lines in the Debye–Scherrer pattern corresponded to those of $LiVO_3$.

Crystals were analyzed for lithium and vanadium using atomic absorption spectrophotometry. The lithium content was found to be somewhat low, however, since the error of the method is relatively large and compounded by small sample sizes and low weight percentage of lithium, the results are consistent with stoichiometric formulations for the phases. The TGA results, however (see below), do provide strong evidence that the phases are lithium deficient and that the oxidation state of vanadium is higher than 3+.

Magnetic susceptibilities in the temperature region 80–610 K were measured using the Faraday method with a Cahn microbalance, and diamagnetic corrections were incorporated.

Results and Discussion

SEM photographs of hexagonal platelet-type and octahedral-type $LiVO_2$ crystals are given in Fig. 1. The octahedral-type crystals grow in a dendritic manner, vertex within vertex. The dendrites frequently occurred in parallel arrays perpendicular to and growing out of other dendrites. The cathode surface within and immediately above the flux was thoroughly embedded

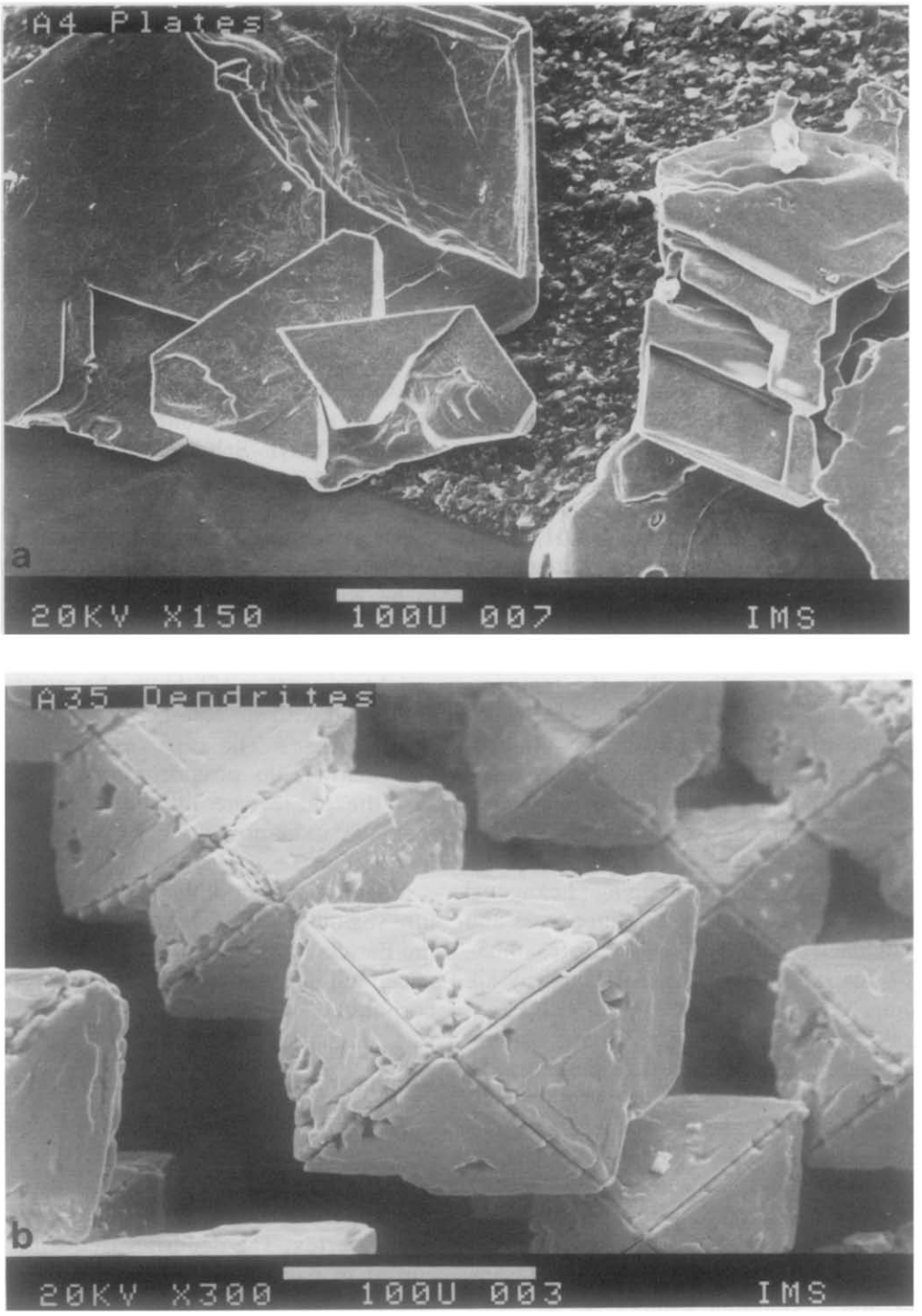

FIG. 1. SEM photographs of (a) hexagonal platelet-type, and (b) dendritic octahedral-type $LiVO_2$ crystals.

with small octahedra. Both types of crystals are brilliantly black in reflected light; their Gandolfi and Debye–Scherrer X-ray diffraction patterns are virtually identical. Figure 2 shows the very similar X-ray diffraction patterns of powdered samples of the two types of crystals, and of $LiVO_2$ powder. All three patterns can be indexed in the trigonal system, except for the very weak reflection near 11°, with the following hexagonal unit cell dimensions: dendrites, a = 2.842(1), c = 14.732(9) Å; platelets, a = 2.842(1), c = 14.758(6) Å; powder, a = 2.841(1), c = 14.75(1) Å. The latter values agree well with those previously reported for $LiVO_2$ powder (*1, 7*). The resulting specific volumes for the three phases are 34.35, 34.41, and 34.37 $Å^3/Z$, respectively.

The DSC curves for a sample of dendrites are given in Fig. 3, and show the semireversible phase transition slightly above 150°C. During the first heating cycle the transition temperature and the associated absorbed heat are significantly higher than in following cycles. This effect is observed in both types of crystals and also in $LiVO_2$ powder. The second and subsequent heating cycles give essentially identical thermal profiles. The enthalpies measured in the present study for the various forms of $LiVO_2$ were in the range 500–1000 cal/mol. This quantity of heat is similar to that associated with the phase transition in VO_2 near 70°C (800 cal/mol), but is very different from the previously reported values for $LiVO_2$ (83 cal/mol; 30 kcal/mol (*5*)).

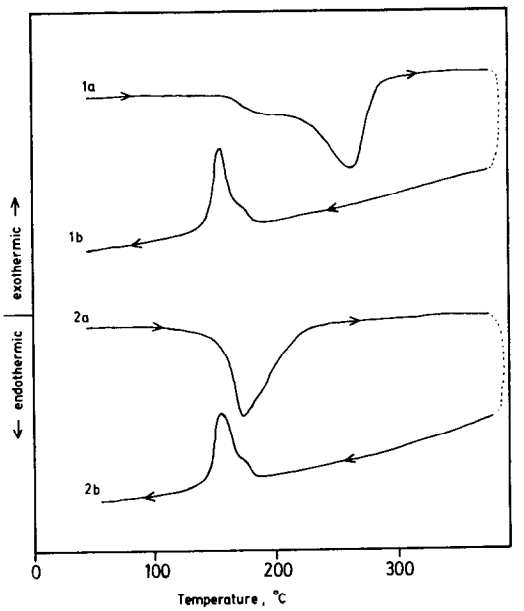

FIG. 3. DSC curves for dendritic octahedral-type $LiVO_2$ crystals: (1a) Cycle 1, heating (ΔH = 1060 cal/mol); (1b) Cycle 1, cooling; (2a) Cycle 2, heating (ΔH = 740 cal/mol); (2b) Cycle 2, cooling.

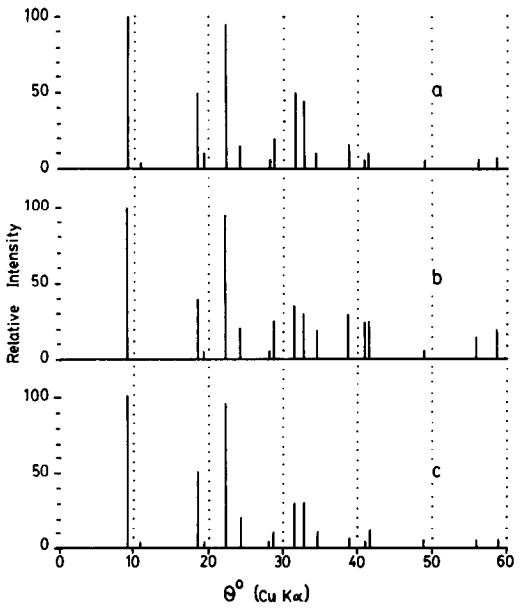

FIG. 2. Debye–Scherrer X-ray diffraction patterns for (a) octahedral-type dendritic $LiVO_2$ crystals; (b) hexagonal platelet-type $LiVO_2$ crystals; (c) $LiVO_2$ powder.

The TGA curve for a sample of dendrites is given in Fig. 4 and is essentially identical to those obtained for the platelet-type crystals and $LiVO_2$ powder. Oxidation of the samples was accompanied by the following weight increases: dendrites, 14.8%; platelets, 14.9%; powder, 15.1%. These results and the very similar specific volumes obtained from the crystallographic data are

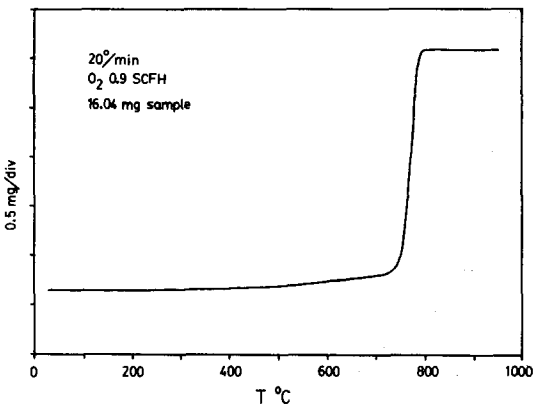

FIG. 4. TGA curve for dendritic octahedral-type $LiVO_2$ crystals.

consistent with the three phases having nearly identical stoichiometries. As the calculated weight increase in the conversion of $LiVO_2$ to $LiVO_3$ is 17.8%, the TGA results are also a strong indication of nonstoichiometry and the presence of V^{4+} in addition to V^{3+}. The authors' observation of an EPR signal from $LiVO_2$ powder is also consistent with the presence of V^{4+}. The formula Li_xVO_2 with $x = 0.6$–0.7 is consistent with the TGA results.

The magnetic susceptibility of a sample of dendritic crystals as a function of temperature for three heating cycles is given in Fig. 5. The phase transition is accompanied by a sharp increase in susceptibility and the resultant curve is very similar to that reported in the literature for $LiVO_2$ powder (*2, 3, 5, 6*), except for the uniqueness of the first heating cycle, which has until now not been reported. The effective magnetic moment varies from a low value of 0.64 μ_B at the start of the first heating cycle to 1.92 μ_B at 600 K. Heating through the transition region is accompanied by a marked increase in the moment from 1.1 to 1.7 μ_B.

X-Ray precession photographs were taken of a platelet using long-exposure times of several days. A superstructure was indicated by the presence of weak reflections in addition to fundamental reflections consistent with a parent structure of the α-$NaFeO_2$-type (space group $R\bar{3}m$). Indexing only the fundamental reflections indicated hexagonal cell dimensions $a' = 2.86$, $c = 14.85$ Å which are in agreement with the values obtained in the refinement of the powder data. Upper level symmetry, however, was found to be C_{6l} rather than C_{3l} which is expected for a $\bar{3}m$ Laue group. In order to account for all of the weak reflections, a larger hexagonal cell was indicated

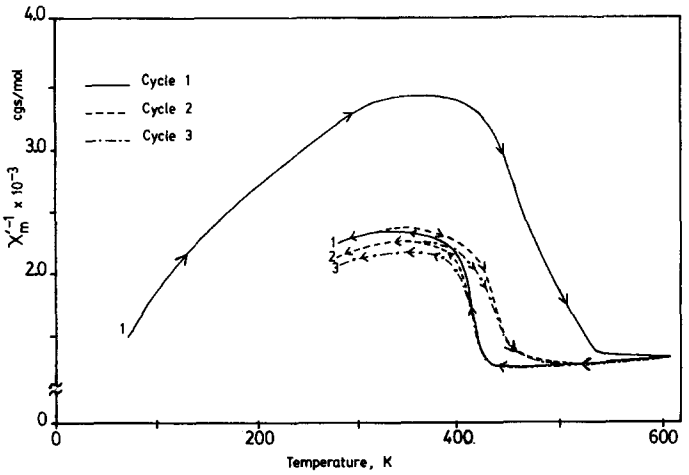

FIG. 5. Inverse magnetic susceptibility versus temperature for $LiVO_2$ octahedral-type dendritic crystals; arrows indicate heating or cooling portion of cycle.

having $a = 2\sqrt{3}a' = 9.94$, $c = 14.85$ Å. The systematic absences were consistent with the space groups $P6_222$ and $P6_422$. The Debye–Scherrer data for the powdered platelets (Fig. 2b) were refined by assigning indices based on the precession photographs, yielding cell dimensions $a = 9.838(4)$, $c = 14.755(6)$ Å.

Precession photographs of a large octahedral-type crystal were anomalous in appearance. The zero-level symmetry taken along a crystal vertex was 4_1 as was the upper level symmetry in two directions 90° apart. The data indicate a "pseudocubic" face-centered unit cell with approximate cell edge 8.2–8.3 Å. Doubling of certain reflections was observed, most notably the (440)-type. The doubling is symmetrical but selective, and the doublets in the (440) region correspond to *d*-values of 1.42 and 1.47 Å, seen as moderately strong reflections at 31.6 and 32.9° in Fig. 2a. With the exception of four weaker reflections, the powder data in Fig. 2a can be refined on the basis of a face-centered cubic unit cell with edge 8.31(1) Å. This cell dimension is similar to that obtained for atacamite-type $LiVO_2$ ($a = 8.227(2)$ Å, space group $Fd3m$ (7)); however, the powder diffraction patterns for these two phases are somewhat different.

Comparison of theoretical powder diffraction patterns calculated for cubic atacamite-type $LiVO_2$ ($a = 8.30$ Å, $Fd3m$) and trigonal α-$NaFeO_2$-type $LiVO_2$ ($a = 2.84$, $c = 14.80$ Å; $R\bar{3}m$) indicates that only small differences are expected. This is a result of two factors. First, the X-ray scattering factor for Li^+ is very small—complete removal of Li^+ from the structure in the theoretical calculations yields a predicted powder pattern that is almost unchanged. Second, in the atacamite-type structure, the two cations still remain largely segregated on alternating (111)-type planes (67%), hence the atacamite version could be regarded as a slightly disordered, ordered variant of the trigonal form. In any case, both versions are closely related to a common prototypical rock salt-type structure.

The precession photographs for both the platelet- and octahedral-type crystals indicate that the crystallinity of these phases is somewhat poor; diffraction spots are broadened and diffuse. The preparation of the crystals involves cooling through the transition region which could lead to extensive fracturing and/or domain formation. The octahedral-type crystals are quite fragile and are easily crushed between glass slides with the slightest pressure. Genuine disorder and/or fine-scale twinning of short-range-order crystals could exist. The different morphologies observed for the two types of crystals in conjunction with the striking similarities in their X-ray powder diffraction patterns indicate that crystal growth could have occurred under slightly different conditions and/or that structural differences may be very slight. Further investigation of these structural differences may shed light on the nature of the phase transition.

References

1. W. Rüdorff and H. Becker, *Z. Naturforsch, B* **9,** 613, 614 (1954).
2. P. F. Bongers, Ph.D. dissertation. The University of Leiden, Leiden, The Netherlands, 1957.
3. P. F. Bongers, *in* "Crystal Structure and Chemical Bonding in Inorganic Chemistry" (C. J. M. Rooymans and A. Rabenau, Eds.), Chap. 4, Elsevier, New York (1975).
4. B. Reuter, R. Weber, and J. Jaskowski, *Z. Elektrochem.* **66,** 832 (1962).
5. K. Kobayashi, K. Kosuge, and S. Kachi, *Mater. Res. Bull.* **4,** 95 (1969).
6. J. B. Goodenough, "Magnetism and the Chemical Bond," p. 269, Interscience, New York (1963).
7. C. Chieh, B. L. Chamberland, and A. F. Wells, *Acta Crystallogr. Sect. B* **37,** 1813 (1981).
8. D. W. Murphy, M. Greenblatt, S. M. Zahurak, R. J. Cava, J. V. Waszczak, G. W. Hull, and R. S. Hutton, *Rev. Chim. Miner.* **19,** 441 (1982).
9. J. Andrieux and H. Bozon, *C.R. Acad. Sci. (Paris)* **230,** 953 (1950).